Title

THE ROLE OF WETTABILITY IN THE BREAK-UP OF LIQUID FILMS INSIDE CONSTRICTED CAPILLARIES

Authors

Gauglitz, P.A.
Radke, C.J.

Publication Date

1986-06-01

Lawrence Berkeley Laboratory
UNIVERSITY OF CALIFORNIA

EARTH SCIENCES DIVISION

Presented at the 190th ACS National Meeting,
Chicago, IL, September 8-13, 1985

THE ROLE OF WETTABILITY IN THE BREAK-UP OF LIQUID FILMS INSIDE CONSTRICTED CAPILLARIES

P.A. Gauglitz and C.J. Radke

June 1986

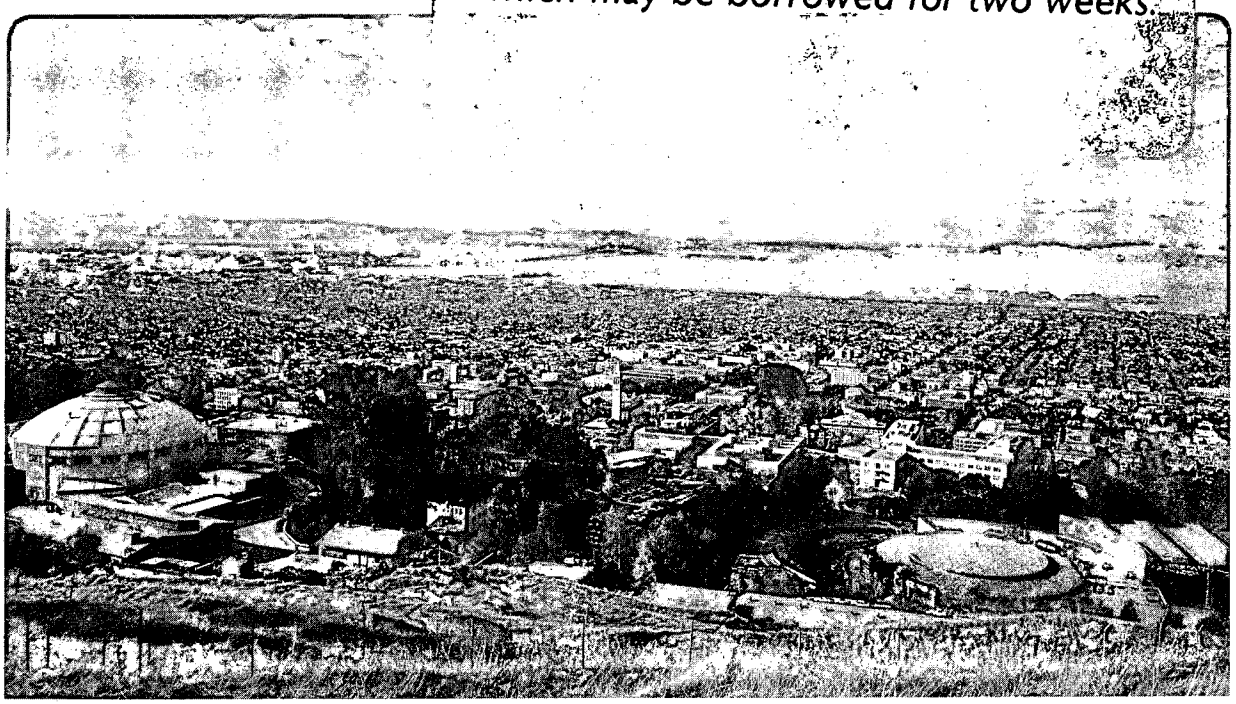

Prepared for the U.S. Department of Energy under Contract DE-AC03-76SF00098

DISCLAIMER

THE ROLE OF WETTABILITY IN THE BREAK-UP OF LIQUID FILMS INSIDE CONSTRICTED CAPILLARIES

P.A. Gauglitz[1] and C.J. Radke[1,2]

[1]Chemical Engineering Department
University of California
Berkeley, California 94720

[2]Earth Sciences Division
Lawrence Berkeley Laboratory
University of California
Berkeley, California 94720

June 1986

This work was supported by the U.S. Department of Energy through Contract No. DE-AC03-76SF00098.

The Role of Wettability in the Break-up of Liquid Films Inside Constricted Capillaries

P. A. Gauglitz and C. J. Radke

Department of Chemical Engineeering

University of California

Berkeley, California 94720

ABSTRACT

To understand the role of wettability on gas-foam generation in porous media, this work considers the effect of conjoining/disjoining pressure on the dynamics of a liquid film forming an unstable collar in both straight and constricted cylindrical capillaries. A hydrodynamic lubrication analysis is presented to describe the time evolution of a thin viscous film under the influence of surface tension and the conjoining or disjoining forces. Time to break-up depends on the pore shape, the strength of the conjoining/disjoining forces, the initial film thickness, and also, on the fluid viscosity, interfacial tension, and unconstricted pore radius which combine to form a characteristic scaling time.

Results show that both conjoining (intermediate wettability) and disjoining (strongly wetting) forces inhibit break-up. We propose the criterion that these forces inhibit snap-off when $Ca \leq |3A^*/\sigma R_T^{*2}|^{3/8}$, where A^* is proportional to the Hamaker constant and σ denotes the surface tension. Thus, wettability inhibits snap-off at very low bubble capillary numbers, Ca, or in very small radius capillaries, R_T^*.

1. INTRODUCTION

Thin liquid films wetting solid surfaces arise in many physical situations. Of primary interest here are oil-bearing underground porous media. When two phases are present in a porous medium, the distribution of the wetting and nonwetting phases within the pore spaces is crucial to the motion of these fluids (Scheidegger, 1974). Often, wetting liquid flows into collars at pore constrictions that may become unstable and snap-off to form liquid lenses (Mohanty, 1981). The lenses (i.e., liquid lamellae), if stabilized by surfactants, may block flow paths and increase the resistance to flow through the porous medium. Foam occurs in the porous medium when large numbers of liquid films break up to form lenses which are stabilized against rupture. The addition of surfactants, to stabilize the lenses, is known to improve mobility control and reduce gravity override in steam displacement processes for increasing heavy oil recovery (Dilgren & Deemer, 1982; Ploeg & Duerksen, 1985).

An important mechanism for foam bubble generation is snap-off at pore necks (Mast, 1972). The four key steps in bubble snap-off are depicted in Figure 1. In the first two steps, the nonwetting bubble moves through a liquid-filled constriction depositing a film of wetting liquid. Due to a difference in interfacial curvature, liquid is driven into the growing collar by surface tension forces as shown in step 3. Eventually, sufficient liquid collects in the collar and it becomes unstable and breaks up to form a liquid lens as shown in step 4. This final step is bubble snap-off to form a foam lamella.

The objective of this work is to determine how wettability influences the above snap-off mechanism in constricted cylindrical capillaries. By wettability we refer here to the macroscopic, static contact angle, θ, gauged through the liquid phase. Contact angles less than 90° reflect partial wetting while those greater than 90° correspond to partial nonwetting. Complete wetting and nonwetting occurs at 0° and 180° contact angles.

As shown by Ivanov and co-workers (1978), and Mohanty (1981), and discussed by others (Martynov & co-workers, 1976; Deryagin & co-workers 1976), macroscopic wettability is directly related to the molecular conjoining/disjoining pressure. Conjoining and disjoining forces arise in

thin fluid films (e.g., less than 1 μm thick) where the close proximity to a solid wall modifies the pressure in the liquid film. Deryagin (Deryagin & Kussakov, 1939; Clunie & co-workers, 1971) defined the disjoining pressure as the excess pressure arising in thin films above the pressure of the same fluid as a bulk phase. A positive disjoining pressure corresponds to a lower pressure in the film than the same fluid in its bulk state. This situation leads to a spontaneous thickening of the film. With a liquid film and a positive disjoining function, complete wetting (i.e. $\theta = 0$) occurs. Conversely, a negative disjoining pressure, called conjoining pressure, corresponds to a higher pressure in the film. Here, local thinning of the film occurs which eventually leads to dewetting of the solid surface (Ruckenstein & Jain, 1974; Williams & Davis, 1982; Kheshgi, 1984). For a liquid film with a negative disjoining function, contact angles greater or equal to 90^o arise. This results in partial nonwetting and a gas film adjacent to the solid surface.

Disjoining and conjoining forces also play a role in the dynamics of the snap-off phenomena. Teletzke (1983) has shown that the conjoining/disjoining pressure alters the film thickness deposited by a bubble. This result is important since the film thickness governs the rate of liquid flow into the growing collar shown in step 3 of Figure 1. In addition, the flow rate in the liquid film must also be influenced by the conjoining/disjoining pressure. Therefore, we include conjoining/disjoining forces when describing the film flow depicted in Figure 1. This permits us to investigate the role of liquid wettability during gas bubble snap-off in constricted cylindrical capillaries.

2. PREVIOUS WORK

The shape and static stability of wetting collars (Figure 2a) has been investigated by Everett and Haynes (1972) and Mohanty (1981). Their results show that thin collars are stable, but sufficiently thick collars are unstable and break-up into lenses, Figure 2b. Mohanty (1981) considered straight and constricted capillaries, and included disjoining and conjoining forces in his analysis. For a fixed capillary pressure (i.e., the pressure difference across the collar interface due to the curvature and the conjoining/disjoining pressure), Mohanty found that pure disjoining forces stabilize an otherwise unstable collar, and conversely, a combination of disjoining and

conjoining forces (partial wetting) destabilize an otherwise stable collar. These static results are useful, but to determine the size and rate of bubbles generated by snap-off we must consider the dynamics of collar growth and break-up.

Dynamic break-up of liquid films in straight capillaries (when conjoining/disjoining forces are negligible) has also received attention. The initial linear stability analysis performed by Goren (1962) demonstrates that infinitesimal sinusoidal disturbances grow exponentially in liquid films of uniform thickness wetting the inside wall of a capillary. This is in accordance with the experimental data of Goren (1962), Goldsmith and Mason (1963), and Gauglitz (1986). More recently, Hammond (1983) developed a nonlinear analysis, restricted to films that are thin compared to the capillary radius, to follow the fate of disturbances when their amplitude becomes large. Since the film thickness must be small compared to the capillary radius, Hammond's solution only permits films to evolve into stable collars such as the one depicted in Figure 2a. Thus, Hammond's analysis unfortunately does not permit break-up, which is step 4 in Figure 1. The experimental data of Goren (1962), Goldsmith & Mason (1963), and Gauglitz (1986) clearly show that liquid films indeed do break-up into lenses, such as the one depicted in Figure 2b. The inadequacy of Hammond's thin-film approximation lies in the inaccurate estimate of the circumferential curvature during the latter stages of the break-up to form the liquid lens. In this paper, we employ an extended evolution equation utilizing a more correct estimate of the circumferential curvature (Gauglitz & Radke, 1986a; Gauglitz, 1986), in addition to including conjoining and disjoining forces.

The influence of conjoining/disjoining pressure on the motion of liquid films in cylindrical geometries, the main theme of this work, has not been very thoroughly examined. Jo (1984) considered the stability of an annular film in straight capillaries by employing directly the results of Ruckenstein and Jain (1974). However, only liquid motion on a planar solid surface was considered by Ruckenstein and Jain. Thus, Jo neglects completely the crucial circumferential curvature in his analysis. Both Hammond (1983) and Goren (1962) show that the growth of disturbances is influenced by the delicate competition between the transverse and circumferential radii

of curvature. Therefore, we include here both principle radii of curvature and the conjoining/disjoining pressure in our analysis.

In section 3, we derive a nonlinear evolution equation for axisymmertric liquid films in constricted capillaries. To provide useful physical insight into the role of fluid wettability in the break-up process, section 4 presents a linear stability analysis in the thin-film limit of the evolution equation for straight capillaries. Section 5 gives the full numerical solution to the nonlinear evolution equation for liquid films in constricted capillaries. Finally, since conjoining/disjoining forces influence both the deposited film thickness and the evolution of the film, section 6 elucidates the combined effect of these two phenomena on bubble snap-off, and summarizes the role of wettability.

3. THEORY

Consider a viscous film of liquid wetting the inside wall of a constricted capillary, as shown in Figure 3. Cylindrical coordinates (r,x) are used with the axial origin at the neck of the constriction. The radius of the unconstricted pore is R_T^*. The shape of the constriction is prescribed by an arbitrary function, $\lambda(x)$, whose slope is small so the radius of the capillary changes slowly with position. Variables and dimensions in Figure 3 are nondimensionalized as follows:

$$r = r^*/R_T^* \qquad x = x^*/R_T^* \ , \tag{1}$$

$$p = p^*/(\sigma/R_T^*) \quad \Pi = \Pi^*/(\sigma/R_T^*) \ , \tag{2}$$

$$\tau = t^*/(3\mu R_T^*/\sigma) \ , \tag{3}$$

$$\kappa = r^*/R_T^* = \lambda - h \qquad at\ the\ interface \ . \tag{4}$$

The superscript * represents dimensional quantities; all unsuperscripted quantities are dimensionless. Time is scaled by a characteristic time obtained from ratio of the length R_T^* over the characteristic velocity σ/μ Hammond (1983). The important unknown is κ, the radial position of the film interface, or equivalently h, the local film thickness. For the results reported here, we define the pore shape with a cosine function as follows:

$$\lambda(x) = 1 - 0.4\left[1 + cos\,(x\,\pi/10)\right]. \tag{5}$$

To follow the liquid motion in the film, a nonlinear evolution is derived for the dynamic film

position κ (Atherton & Homsy, 1976; Hammond, 1983). We utilize here, an extension of the small-slope evolution equation proposed by Gauglitz (1986), and Gauglitz and Radke (1986b) to include conjoining/disjoining pressure.

According to Figure 3, liquid flows in the film due to a gradient in the mean curvature of the interface along the capillary, and also due to a gradient in the disjoining pressure arising from variations in the film thickness. If the film is thin and the slope of the pore wall is small, the classical lubrication approximation applies for the fluid motion in the film. In addition, inertial effects are neglected (Hammond, 1983), and rectangular coordinates are employed. We modify the equations of motion by including the conjoining/disjoining forces as a body force (Williams & Davis, 1982; Chen and co-workers, 1984). Within the lubrication approximation, Teletzke (1983) has justified this approach theoretically. The velocity profile, v_x^* in Figure 3, is determined easily after imposing the boundary conditions of no-slip at the capillary wall, and no-stress at the gas-liquid interface, since the gas is presumed inviscid. Integrating the velocity profile over the thickness of the film gives the volumetric flow as a function of the total pressure driving force as follows:

$$\frac{Q^*}{R_T^* \sigma/\mu} = \lambda \left[-\frac{\partial p}{\partial x} + \frac{\partial \Pi}{\partial x} \right] h^3 \ , \tag{6}$$

where Π is the nondimensional conjoining/disjoining pressure. The following simple functional form for the disjoining pressure (Kruyt, 1952) proves sufficient for this investigation:

$$\Pi^*(h^*) = \begin{cases} -A^*/h^{*3} & conjoining \\ A^*/h^{*3} & disjoining \end{cases} , \tag{7}$$

where $\pm A^*$ is a dimensional scaling coefficient. A^* is related to the Hamaker constant and typically has values near 10^{-21} J (Kruyt, 1952). Other simple functional forms are available for Π, such as an inverse quadratic or an exponential dependence on the film thickness (Kruyt, 1952; Mohanty, 1981; Teletzke, 1983; Jo, 1985).

As noted above, Ivanov and co-workers (1978) and Mohanty (1981) have shown that the conjoining/disjoining pressure determines the contact angle. If the disjoining pressure is always greater than zero, the liquid-phase contact angle is zero. However, for a conjoining/disjoining

pressure function which is both positive at small film thicknesses, and negative at larger thicknesses, intermediate wettability exists with a contact angle θ of $0 < \theta < \pi/2$. The disjoining pressure functions given by Equation 7, correspond to a perfectly wetting liquid ($\theta = 0$) for $+A^*/h^{*3}$. Following the analysis of Mohanty (1981), we find that the conjoining pressure function, $-A^*/h^{*3}$, results in $\theta \geq \pi/2$, which is a partially to completely nonwetting liquid. Although simple, the inverse cubic dependence for the conjoining/disjoining pressure given by Equation 7 represents both wetting and nonwetting liquids, and will suffice here.

The pressure driving force in Equation 6 is obtained from the normal stress balance at the film interface, which is the Young-Laplace equation within our approximation. We impose the following small-slope approximation to the curvature which was proposed by Gauglitz (1986) and Gauglitz and Radke (1986b) as a simple, yet accurate approximation:

$$-p = \frac{1}{\kappa} - \frac{\partial^2 \kappa}{\partial x^2} \ , \tag{8}$$

where p is the liquid pressure, and the gas pressure is set to zero since it is assumed constant.

To obtain an evolution equation, we combine the derivatives of Equations 7 and 8 with an integral form of the continuity equation and the kinematic condition (Teletzke, 1983; Hammond, 1983), and substitute the flow relation, Equation 6, to yield:

$$\frac{\partial \kappa}{\partial \tau} = \frac{1}{\kappa}\frac{\partial}{\partial x}\left\{\left[-\frac{1}{\kappa^2}\frac{\partial \kappa}{\partial x} - \frac{\partial^3 \kappa}{\partial x^3} + 3\tilde{A}\frac{1}{(\lambda-\kappa)^4}\left(\frac{d\lambda}{dx} - \frac{\partial \kappa}{\partial x}\right)\right]\lambda(\lambda-\kappa)^3\right\} \ , \tag{9}$$

where $\tilde{A} = \pm A^*/(\sigma R_T^{*2})$ is a dimensionless measure of the conjoining/disjoining pressure. This group is sometimes refer to as the Scheludko number (aside from a factor of $1/6\pi$; Gumerman & Homsy, 1975).

Equation 9 is the desired evolution equation for the dynamic interface position in a constricted capillary. This equation is a highly nonlinear partial differential equation that is first order in time and fourth order in axial position. We must further simplify this relation to obtain analytic information, otherwise, the only amenable solution is numerical. To give useful physical insight, we consider now a linear stability analysis of the proposed evolution equation, Equation 9.

4. LINEAR STABILITY ANALYSIS

Qualitative understanding of the role of conjoining/disjoining forces emerges by considering the fate of infinitesimal sinusoidal disturbances with a normal modes analysis (Drazin and Reid, 1981; Williams & Davis, 1982; Hammond, 1983). To obtain a simple base state, we consider only a straight capillary with a wetting film of uniform thickness initially at rest. As a further simplification, we adopt only the thin-film limit of the evolution equation (Hammond, 1983; Gauglitz, 1986) obtained by substituting for κ in Equation 9 the following:

$$\kappa = 1 - \epsilon \bar{h} \quad , \tag{10}$$

where ϵ is a small constant reflecting the initial film thickness in the straight capillary, and $\bar{h} = h^* / h_o^*$ is a scaled film thickness. Expanding in a Taylor series for $\epsilon \rightarrow 0$ and keeping leading order terms in ϵ gives:

$$\frac{1}{\epsilon^3}\frac{\partial \bar{h}}{\partial \tau} = -\frac{\partial}{\partial x}\left\{ \bar{h}^3 \left[\frac{\partial^3 \bar{h}}{\partial x^3} + \frac{\partial \bar{h}}{\partial x} + \frac{3\tilde{A}}{\epsilon^4}\frac{1}{\bar{h}^4}\frac{\partial \bar{h}}{\partial x} \right] \right\} . \tag{11}$$

This is a direct extension of Hammond's (1983) nonlinear evolution equation to include conjoining/disjoining forces. Consider now sinusoidal disturbances of the form,

$$\bar{h} = 1 + \beta e^{\alpha \tau + ikx} \quad , \tag{12}$$

where β is a small constant reflecting the amplitude of the infinitesimal disturbance. Substituting Equation 12 into Equation 11 and linearizing yields the following dispersion relation:

$$\frac{\alpha}{\epsilon^3} = -k^4 + k^2\left(1 - 3\frac{\tilde{A}}{\epsilon^4}\right) \quad , \tag{13}$$

where α is the growth rate factor. That is, instabilities grow only for positive α values. The wavelength of the fastest growing disturbance, Λ_{max} is by

$$\Lambda_{max} \equiv 2\frac{\pi}{k_{max}} = \frac{2^{3/2}\pi}{\left(1 - \frac{3\tilde{A}}{\epsilon^4}\right)^{1/2}} . \tag{14}$$

4.1. RESULTS: LINEAR STABILITY

The linear analysis determines whether sinusoidal disturbances grow or decay. As portrayed in Figure 4, the dispersion relation (Equation 13) gives a one parameter family of curves relating

the dimensionless growth rate to the wavelength of the disturbance. At each parameter value, the maximum in the curve corresponds to the fastest growing disturbance which dominates the film breakup. The crucial parameter determining the role of conjoining/disjoining pressure is $3\tilde{A}/\epsilon^4$ which shows the important influence of the initial film thickness ϵ and the size of the pore, R_T^*, since $\tilde{A} = A^*/(\sigma R_T^{*2})$. For $3\tilde{A}/\epsilon^4 = 0$, we recover the results of Hammond (1983) where $\Lambda_{max} = 2^{2/3}\pi$.

Conjoining/disjoining pressure affects the both the value of the growth-rate parameter and the wavelength of the fastest growing disturbance. For $0 < 3\tilde{A}/\epsilon^4 < 1$, disjoining pressure resists local thinning of the film, and accordingly, the growth rate is less. The dominate wavelength shifts towards longer waves corresponding to a decrease in the wave number, k. When $3\tilde{A}/\epsilon^4 \geq 1$, all disturbances decay and a stable film uniformly wets the inside wall of the capillary.

Conjoining pressure, corresponding to $3\tilde{A}/\epsilon^4 < 0$, increases the growth rate and shifts the fastest growing disturbance towards shorter wavelengths. Analogous to Ruckenstein and Jain (1974), Williams and Davis (1982), and Kheshgi (1984), the growth of a disturbance indicates the initial dynamics of a thin film evolving to either a dry patch (dewetting) or a liquid lens. Dewetting is detrimental to snap-off as we discuss further in section 5.

When disjoining forces are sufficiently large (i.e., $3\tilde{A}/\epsilon^4 \geq 1$), the liquid is strongly wetting: all disturbances are damped since the growth-rate factor defined by Equation 13 is negative for all wavelengths. When $3\tilde{A}/\epsilon^4 << -1$, Equation 13 demonstrates that the conjoining pressure is the dominate driving force for break-up. That is, the factor of unity in the denominator on the right side of Equation 13, which arises from the circumferential radius of curvature, is small compared to the conjoining pressure term. Accordingly, the growth rate α is established by the competition between the stabilizing transverse curvature (*i.e.*, $-k^4$ in Equation 13) and the driving force which is the conjoining pressure (*i.e.*, $-k^2 3\tilde{A}/\epsilon^4$ in Equation 13). For this limiting situation, our results simplify to those of Jo (1984) and Ruckenstein and Jain (1974) since the geometry is now essentially planer. The nonlinear analysis of Williams and Davis (1982) applies in this limit-

ing case as well.

The important results of the linear stability analysis is that disjoining pressure makes all disturbances stable if $3\tilde{A}/\epsilon^4 \geq 1$, and that conjoining forces become important when $3\tilde{A}/\epsilon^4 \leq -1$. Combining these criteria we find that conjoining/disjoining pressure must be considered when $3|\tilde{A}|/\epsilon^4 \geq O(1)$.

The linear stability analysis also demonstrates that two types of break-up exist: 1) snap-off due to the circumferential curvature, and 2) spontaneous film rupture (i.e., dewetting) due to the conjoining pressure. The linear stability analysis can not determine which type of break-up will predominate, snap-off or dewetting, since it only indicates whether infinitesimal sinusoidal disturbances grow or decay. To determine which occurs first, snap-off or dewetting, we must perform a nonlinear stability analysis which involves solving Equation 9.

5. NONLINEAR EVOLUTION

Consider the evolution of a film of uniform thickness coating the inside wall of a smoothly constricted capillary as prescribed by Equation 5. Since conjoining/disjoining forces depend on the thickness of the film, a range of initial thicknesses is investigated. In addition to the conjoining/disjoining forces becoming more important in thinner films, the time required for liquid to flow into the growing collar depends strongly on the thickness of the liquid film. With thicker films, liquid flows more quickly since viscous resistance is relatively less and collars snap off faster. Conversely, with thinner films, snap-off occurs more slowly since the viscous resistance to flow is larger in the thinner films. This is evident in Equation 6 where the flow rate in the film has a cubic dependence of the film thickness h.

5.1. NUMERICAL SOLUTION

The evolution equation given by Equation 9 demands numerical solution. It is parabolic in nature, requiring an initial condition and four boundary conditions. The initial profile is a film of constant uniform thickness $h_o = h_o^*/R_T^*$ which results in the following initial condition:

$$\kappa(x,0) = \lambda(x) - h_o \quad . \tag{15}$$

Note that h_o in the constricted capillary is equivalent to ϵ in the straight capillary. The boundary conditions of symmetry at the pore neck (x=0) indicates that the first and third derivatives are zero:

$$\frac{\partial \kappa(x,\tau)}{\partial x} = \frac{\partial^3 \kappa(x,\tau)}{\partial x^3} = 0 \quad at \ x = 0 \ . \tag{16}$$

A long distance from the pore we require that the film have a constant thickness and zero slope:

$$\kappa(x,\tau) = 1 - h_o \ , \quad \frac{\partial \kappa(x,\tau)}{\partial x} = 0 \quad at \ x = +16 \ . \tag{17}$$

At a position of $x = +16$, the boundary conditions given by Equation 17 have no influence on the collar evolution. Applying the boundary conditions of Equation 17 further away from the constriction causes no change in the results indicating that indeed x = +16 is a long distance from the constriction. In addition, we have investigated applying symmetry conditions at x = +16 where the first and third derivatives are zero as in Equation 16. There is no difference in the results so our analysis applies to periodically constricted capillaries as well.

To obtain a numerical solution, we employ the Galerkin finite element method (Becker, Carey & Oden, 1981; Finlayson, 1980) to discretize the axial derivatives in Equation 9, and the Crank-Nicholson method (Lapidus, 1962) to discretize the time derivatives. The resulting system of nonlinear algebraic equations is solved at each time step with Newton-Raphson iteration. Extensive details of the numerical procedures are given in Gauglitz (1986). We report next, the results for a range of initial thickness which show the influence of conjoining/disjoining forces.

5.2. RESULTS: CONSTRICTED CAPILLARY

We focus on the effect of the initial film thickness because of its strong influence on the time to break-up. Time to break up is defined as the instant when the collar crosses the centerline of the pore. Collar growth accelerates rapidly at the end of the break-up process, and the calculation is stopped before the neck radius of the collar becomes identically zero. Interrupting the calculation when the collar neck radius becomes less than $0.05R_T^*$ gives an error of less than 1% in the calculated time to break-up. Rapid growth of the collar once it reaches a critical thickness has been elucidated in a previous study (Gauglitz, 1986; Gauglitz & Radke, 1986b) and is observed

experimentally (Goldsmith & Mason, 1963). Results without thin-film forces will be discussed first, then the effects of conjoining/disjoining forces are included.

The initial condition of a uniform initial film along the pore wall is shown in Figure 5. A sequence of film profiles is shown in Figure 6 for a uniform initial film of thickness $h_o = 0.0124$ with $\tilde{A}$ set to zero. To observe the collar shape more carefully, we plot the solution only near the constriction neck. The first profile at $\tau = 1500$ shows the initial film growing thicker at the pore neck as liquid collects in a growing collar. In the second and third profiles local thinning at the sides is noticeable as the collar becomes large. This arises from the collar drawing liquid in rapidly from the sides as the collar accelerates its growth. Indeed, the collar grows at an ever increasing rate as it becomes larger, with break-up occurring at $\tau_b = 5496$, which is soon after the third profile in Figure 6 at $\tau = 5300$.

The effect of the initial film thickness on the time to break up, without conjoining/disjoining forces, is summarized in Figure 7 by the line labeled by $\tilde{A} = 0$. Time to break-up increases rapidly for thinner initial films due to the cubic dependence of the flow in the film on the film thickness as given in Equation 6.

When $\tilde{A}$ is positive, disjoining pressure resists local film thinning and slows collar growth. If sufficiently strong, disjoining pressure completely inhibits snap off. The dynamic evolution results for $\tilde{A} = 3.33(10^{-6})$ are shown in Figure 8 for an initial thickness of $h_o = 0.01$. Although the collar forms slower under the influence of disjoining forces, it eventually does snap-off. The initial profile at $\tau = 0$ shows the uniform initial thickness. At $\tau = 3.0(10^4)$ liquid fills in at the constriction. The collar continues to grow as liquid flows in from the sides of the capillary, as seen in the profiles. However, in comparison to the profiles without disjoining pressure, more liquid fills in before the short-wavelength collar emerges in the film. This can be understood from the linear stability analysis and Figure 4. When disjoining forces become important, the maximum in each curve of Figure 4 decreases (and shifts to small wave numbers). This maximum corresponds to the fastest growing wavelength which now grows slower compared to when $\tilde{A} = 0$. Hence, the collar in Figure 8 emerges slower from the thickening film. Further, the local thinning at the

sides of the collar is inhibited by the disjoining pressure which resists thinning. Thus, the small dips apparent at the side of the collar in Figure 6 (where $\tilde{A} = 0$) do not occur at the sides of the collar in Figure 8.

For comparison, results for different $\tilde{A}$ values are summarized in Figure 7. For positive values of $\tilde{A}$, disjoining pressure increases the time to break-up when the initial film thickness decreases below a critical value. As expected, for larger $\tilde{A}$ (such as a smaller radius capillary), the film thickness when disjoining pressure becomes important is larger than when $\tilde{A}$ is smaller. We see this in Figure 7 by the curve for $\tilde{A} = 1.33(10^{-5})$ deviating from the $\tilde{A} = 0$ curve at a larger initial film thickness than the curve for $\tilde{A} = 3.33(10^{-6})$. When disjoining forces dominate, they completely inhibit snap-off. The liquid film is stable since a collar will not grow, and accordingly, the break-up time becomes infinite. This feature is also apparent from the linear stability analysis (Equation 13). When $\tilde{A}$ is positive (disjoining pressure) and sufficiently large (i.e., $3\tilde{A}/\epsilon^4 \geq 1$), the growth rate is always negative, dictating a stable film. This corresponds to an break-up time becoming infinite in Figure 7. We can further compare the nonlinear results in Figure 7 with the linear stability analysis by noting the equivalence of h_o and ϵ. We find from Figure 7 that disjoining pressure becomes important when $3\tilde{A}/h_o^4 \approx 10$. This is in agreement with the linear stability analysis which gives a criterion of $3\tilde{A}/\epsilon^4 \approx 1$.

When conjoining forces (*i.e.*, $\tilde{A} < 0$) are incorporated into the film evolution, we find that collars grow more rapidly in the initial stages of evolution. This also agrees with the linear stability analysis which demonstrates that conjoining pressure increases the growth rate of a disturbance. Although the linear stability analysis indicates an increases growth rate, it cannot determine which type of break-up will occur: snap-off or dewetting. The numerical solution of the nonlinear evolution equation for constricted capillaries (Equation 9) demonstrates that below a critical initial film thickness, dewetting break-up occurs before snap-off. When conjoining forces are unimportant (smaller $\tilde{A}$ or thicker initial films), snap-off is completely unaffected by the conjoining pressure.

Dewetting begins at the sides of the collar where local thinning occurs, as displayed in Fig-

ure 6. We further depict this thinning and film collapse in Figure 9. Once local thinning begins, conjoining forces drive fluid away from the thin area causing film rupture. This catastrophic event corresponds to dewetting or the formation of a dry patch. As mentioned in section 4, the conjoining pressure function employed (Equation 7) reflects a contact angle of $\theta \geq \pi/2$. Once conjoining collapse occurs, numerical integration of the evolution equation is stopped since we believe the collar will no longer grow because liquid cannot flow into the collar from sides of the capillary. Thus, dewetting inhibits snap-off.

The results including conjoining forces for a series of different negative $\tilde{A}$ values are shown in Figure 7. We indicate with an open circle the critical initial thickness below which dewetting occurs for each value of $\tilde{A}$. As expected, at each negative value of $\tilde{A}$, dewetting occurs for the same initial film thickness at which disjoining forces slow the collar evolution. In accordance with disjoining effects, dewetting occurs in thicker initial films for larger values of $|\tilde{A}|$. It is also apparent in Figure 7 that the time to break-up (i.e., snap-off) is unaffected by the conjoining pressure until dewetting occurs since the curves for all negative $\tilde{A}$ values lie essentially on the curve labeled $\tilde{A} = 0$.

Sections 4 and 5 have considered the affects of conjoining/disjoining forces (wettability) on the dynamic fluid motion in a film that uniformly coats the inside wall on a constricted capillary. The results show that both conjoining and disjoining pressure inhibit snap-off. To complete our study of fluid wettability and snap-off, we must consider the role of conjoining/disjoining pressure as it affects how a liquid film is initially deposited in the capillary; according to step 2 in Figure 1. Teletzke (1983) has shown that when a bubble (or drop) displaces a viscous fluid from a capillary, the thickness of the film deposited by the bubble depends on the conjoining/disjoining pressure. In the next section we combine the results of sections 4 and 5 with the results of Teletzke (1983) to develop criteria for when, and in what manner, fluid wettability affects snap-off.

6. RAMIFICATIONS OF WETTABILITY ON SNAP-OFF

If a bubble or drop displaces a perfectly wetting liquid from a capillary, a film of liquid is deposited on the inside wall of the capillary (Taylor, 1961; Bretherton, 1961). The film thickness

depends on the capillary number which is defined as follows:

$$Ca \equiv \frac{\mu U^*}{\sigma} \quad , \tag{18}$$

where U^* is the velocity of the bubble front. When the bubble (or drop) displaces a fluid of intermediate wettability with $0 < \theta < \pi$ (due to a conjoining pressure contribution), a film of liquid may or may not be deposited. If a liquid film is not deposited, snap-off can never occur.

As indicated in the introduction, the sign and magnitude of the conjoining/disjoining forces determine the fluid wettability (i.e., the contact angle) for static fluid interfaces (Ivanov & co-workers, 1978; Mohanty, 1981), as well as the dynamic contact angle when a gas-liquid interface moves along a solid surface (Teletzke, 1983). Pure conjoining forces cause a liquid to nonwet partially a solid ($\pi/2 \leq \theta \leq \pi$). Conversely, pure disjoining forces indicate complete wetting ($\theta = 0$). With conjoining forces, Teletzke (1983) notes that for bubbles moving through capillaries, there exists a critical capillary number below which no film is deposited, thus preempting the possibility of snap-off. However, for any fluid regardless of its wettability, a liquid film will always be deposited for sufficiently high capillary numbers and snap-off may occur.

Teletzke has calculated the deposited film thickness for the conjoining/disjoining pressure functions given by Equation 7. We can obtain expression for the capillary number (i.e. the film thickness) when conjoining/disjoining pressure becomes important by ascertaining the magnitude of the terms involving the conjoining/disjoining forces in Teletzke's (1983) film-profile equation. Teletzke's equation is given in Appendix A. There we show that conjoining/disjoining pressure becomes important during film deposition if,

$$3|\tilde{A}|\, Ca^{-2} \geq O(1) \quad . \tag{19}$$

We can compare this to the role of wettability in the film evolution. The dispersion relation of the linear stability analysis, Equation 13, and the nonlinear evolution calculations in Figure 7, demonstrate that conjoining/disjoining forces become important when $3|\tilde{A}|/\epsilon^4 \geq O(1)$. The initial film thickness ϵ is related to the capillary number by $\epsilon = O(Ca^{2/3})$ (Bretherton, 1961). Combining these relations, we discover that conjoining/disjoining forces become important during film evolution when

$$3|\tilde{A}|\,Ca^{-8/3} \geq O(1)\ . \tag{20}$$

Notice that Equation 20 has a different capillary number dependence than Equation 19. Comparison shows that for $Ca \ll 1$, conjoining/disjoining forces affect film evolution at a higher capillary number where film deposition remains unaffected.

With Equations 19 and 20, capillary-number criteria can now be developed to predict when snap-off occurs for fluids with any wetting characteristics. We summarize these criteria in Table 1. For conjoining forces, we first consider at what values of the capillary number liquid films are deposited. Equation 19 shows that for $Ca < |\tilde{3A}|^{1/2}$ no film is deposited. We signify this by a "No" in the "Film Deposition" row. In the second row called "Snap-off", we indicate by a "No" that snap-off can never occur without a liquid film. When $Ca > |\tilde{3A}|^{1/2}$ a liquid film is deposited by a bubble (indicated by a "Yes" in Table 1), and a bubble can snap-off. For these higher values of Ca, we must consider the evolution of the film and the role of wettability as given by Equation 20.

For $Ca < |\tilde{3A}|^{3/8}$, a film of liquid is deposited, but it dewets during evolution and does not snap off. Only when $Ca > |\tilde{3A}|^{3/8}$ can a bubble snap off as shown by the "Yes". Snap-off can occur for these values of the capillary number because a finite film of liquid is deposited and during film evolution dewetting does not occur.

For a disjoining force or complete wetting, Table 1 presents Teletzke's (1983) result that a film is deposited at all capillary numbers. However, in the evolution of these films, disjoining forces inhibit snap-off. When $Ca < |3\tilde{A}|^{3/8}$, snap-off does not occur since disturbances will not grow. Conversely, when $Ca > |3\tilde{A}|^{3/8}$, snap-off can occur as indicated by the "Yes".

Since the specific conjoining/disjoining pressure function given by Equation 7 considers both perfectly wetting and partially to completely nonwetting liquids, Table 1 considers all possible combinations of wettability affecting film deposition and evolution. For both disjoining and conjoining forces, snap-off only occurs for $Ca > |3\tilde{A}|^{3/8}$, which implies that a sufficiently thick initial film must be deposited for snap-off to occur.

Experimental results for the time to break-up of gas bubbles moving through constricted capillaries approximately 0.1 cm in diameter are reported elsewhere (Gauglitz, 1986). For parameter values of $A^* = 10^{-21} J$, $\sigma = 30\ mN/m$, and $R_T^* = 5(10^{-4})\ m$, the criteria developed above gives that snap-off can occur if $Ca > 2(10^{-5})$. Thus, wettability inhibits snap-off only at very low capillary numbers. All experiments were performed at Ca values greater than $2(10^{-5})$. The data agree quantitatively with the theory for $\tilde{A} = 0$ indicating wettability is not important in capillaries of this size. In addition, the shape of the growing collar in Figure 6 accurately represents the experimentally observed shape.

For capillary numbers greater than about 10^{-3}, the snap-off criteria dictates that snap-off can occur in pores larger than $1\mu m$. Therefore, wettability inhibits snap-off in cylindrical capillaries only in very small pores. Thus, the calculations presented in this work, and the experimental results in Gauglitz (1986) demonstrate that wettability does not affect snap-off in typical oil-bearing porous media ($R_T^* \approx 10^{-5}\ m$) for capillary numbers greater than 10^{-3}.

Interestingly, other visual observations by Gauglitz (1986) of snap-off in constricted square capillaries indicates that dewetting does occur and inhibits snap-off in 0.1 cm radius capillaries for capillary numbers in the range of 10^{-5} to 10^{-3}. Thus, square capillaries do not follow the criteria developed in section 6. Further study is required to obtain a complete understanding of wettability effects in constricted square capillaries.

7. SUMMARY AND CONCLUSIONS

The role of wettability, as determined by the conjoining/disjoining pressure, on the evolution of liquid films is investigated in both straight and constricted capillaries. Solution of a new nonlinear evolution equation demonstrates that both conjoining and disjoining forces inhibit snap-off. We propose the criterion that gas-bubble snap-off can occur in constricted cylindrical capillaries, unaffected by liquid wettability, if $Ca > |3\tilde{A}|^{3/8}$.

Acknowledgements

This research was supported by the U.S. Department of Energy under contract DE-AC03-765F00098 to the Lawrence Berkeley Laboratory of the University of California. P.A.G. gratefully acknowledges financial support from the Shell Development Company.

Nomenclature

A^* conjoining/disjoining pressure scaling coefficient, $\sim 10^{-21}$ J

$\tilde{A}$ $= A^*/\sigma R_T^{*2}$, dimensionless conjoining/disjoining pressure constant

Ca capillary number (defined in Equation 18)

e $= 2.71828$

h^* film thickness, m

h_o^* initial film thickness, m

h $= h^*/R_T^*$, dimensionless film thickness

h_o $= h_o^*/R_T^*$, dimensionless initial film thickness

$\bar{h}$ $=$ scaled film thickness (defined in Equation 10)

$\tilde{h}$ $=$ scaled film thickness (defined in Appendix A)

i $\sqrt{-1}$

k wave number of sinusoidal disturbance

k_{max} wave number of the fastest growing disturbance

p^* liquid pressure, Pa

p $= p^*/(\sigma/R_T^*)$, dimensionless liquid pressure

r^* radial position, m

r $= r^*/R_T^*$, dimensionless radial position

R_T^* radius of unconstricted capillary, m

t^* time, s

U^* velocity of the bubble front, m/s

v_z^* velocity in fluid film, m/s

x^* axial position, m

x $= x^*/R_T^*$, dimensionless axial position

$\bar{x}$ = scaled axial position (defined in Appendix A)

y^* position from tube wall (see Figure 3), m

Greek Letters

α growth rate factor (defined in Equation 12)

β amplitude of infinitesimal disturbance (defined in Equation 12)

ϵ $= h_o^*/R_T^*$, dimensionless initial film thickness for straight capillary (defined in Equation 10)

θ contact angle through the liquid

κ dimensionless radial position of film interface

λ dimensionless radial position of capillary wall

Λ dimensionless wavelength of disturbance

Λ_{max} dimensionless wavelength of the fastest growing disturbance

μ liquid film viscosity, mPa·s

π 3.14159

Π^* conjoining/disjoining pressure (defined in Equation 7), Pa

Π $= \Pi^*/(\sigma/R_T^*)$, dimensionless conjoining/disjoining pressure

σ surface tension, mN/m

τ $= t^*/(3\mu R_T^*/\sigma)$, dimensionless time

τ_b dimensionless break-up time

References

1. Atherton, R. W. and G. M. Homsy, "On the Derivation of Evolution Equations for Interfacial Waves," *Chem. Engr. Comm.*, vol. 2, pp. 57-77, 1976.

2. Becker, E. B., G. F. Carey, and J. T. Oden, *Finite Elements an Introduction, Volume I,* Prentice-Hall, New Jersey, 1981.

3. Bretherton, F. P., "The Motion of Long Bubbles in Tubes," *J. Fluid Mech.*, vol. 10, pp. 166-188, 1961.

4. Chen, J. -D., P. S. Hahn, and J. C. Slattery, "Coalescence Time for a Small Drop of Bubble at a Fluid-Fluid Interface," *AICHE J.*, vol. 30, no. 4, pp. 662-630, 1984.

5. Clunie, J. S., J. F. Goodman, and B. T. Ingram, "Thin Liquid Films," *in Surface and Colloid Science, ed. Matijevic*, vol. 3, pp. 167-240, Wiley Interscience, 1975.

6. Deryagin, B. V. and M. Kussakov, "Anomalous Properties of Thin Polymolecular Films. V.," *ACTA Physicochimica U.R.S.S.*, vol. 10, no. 1, pp. 25-44, 1939.

7. Deryagin, B. V., V. M. Starov, and N. V. Churaev, "Profile of the Transition Zone Between a Wetting Film and the Meniscus of a Bulk Liquid," *Kolloidnyi Zhurnal*, vol. 38, pp. 875-879, 1976.

8. Dilgren, R. E. and A. R. Deemer, "The Laboratory Development and Field Testing of Steam/Noncondensible Gas Foams for Mobility Control in Heavy Oil Recovery," *SPE 10774*, Presented at the SPE Calif. Regional Meeting, San Francisco, March 24-26.

9. Drazin, P. G. and W. H. Reid, *Hydrodynamic Stability,* Cambridge University Press, New York, 1981.

10. Everett, D. H. and J. M. Haynes, "Model Studies of Capillary Condensation I. Cylindrical Pore Model with Zero Contact Angle," *J. Coll. Int. Sci.*, vol. 38, no. 1, pp. 125-137, 1972.

11. Finlayson, B. A., *Nonlinear Analysis in Chemical Engineering,* McGraw-Hill, New York, 1980.

12. Gauglitz, P. A., "Instability of Liquid Films in Constricted Capillaries: A Pore Level Discription of Foam Generation in Porous Media," *Ph.D. Thesis*, University of California, 1986.

13. Gauglitz, P. A. and C. J. Radke, "An Extended Evolution Equation for Liquid Film Break-up in Cylindrical Capillaries," *in preparation*, 1986a.

14. Gauglitz, P. A. and C. J. Radke, "Dynamics of Gas Bubble Snap-off in a Constricted Capillary," *in preparation*, 1986b.

15. Goldsmith, H. L. and S. G. Mason, "The Flow of Suspensions through Tubes II. Single Large Bubbles," *J. Coll. Sci.*, vol. 18, pp. 237-261, 1963.

16. Goren, S. L., "The Instability of an Annular Thread of Fluid," *J. Fluid Mech.*, vol. 12, pp. 309-319, 1962.

17. Gumerman, R. J. and G. M. Homsy, "The Stability of Radially Bounded Thin Films," *Chem. Eng. Commun.*, vol. 2, pp. 27-36, 1975.

18. Hammond, P. S., "Nonlinear Adjustment of a Thin Annular Film of Viscous Fluid Surrounding a Thread of Another within a Circular Cylindrical Pipe," *J. Fluid Mech.*, vol. 137, pp. 363-384, 1983.

19. Ivanov, I. B., B. V. Toshev, and B. P. Radoev, "On the Thermodynamics of Contact Angles, Line Tension and Wetting Phenomena," *in Wetting, Spreading and Adhesion, ed. J. F. Padday*, Academic Press, London, 1978.

20. Jo, E. J., "Displacement of Bubbles and Drops in Fine Capillaries," *Ph.D. Thesis*, University of Houston, 1984.

21. Kheshgi, H. S., "The Motion of Viscous Liquid Films," *Ph.D. Thesis*, University of Minnesota, 1984.

22. Kruyt, H. R., *Colloid Science*, Elsevier, New York, 1952.

23. Lapidus, L., *Digital Computation for Chemical Engineers*, McGraw-Hill, New York, 1962.

24. Martynov, G. A., I. B. Ivanov, and B. V. Toshev, "On The Mechanical Equilibrium of a Free Liquid Film with the Meniscus," *Kolloidnyi Zhurnal*, vol. 38, pp. 474-479, 1976.

25. Mast, R. F., "Microscopic Behavior of Foam in Porous Media," *SPE 9997*, presented at the 47th Annual Fall Meeting, San Antonio, TX, 1972.

26. Mohanty, K. K., "Fluids in Porous Media: Two-phase Distribution and Flow," *Ph.D. Thesis*, University of Minnesota, 1981.

27. Park, C.-W. and G. M. Homsy, "Two-phase Displacement in Hele Shaw Cells: Theory," *J. Fluid Mech.*, vol. 139, pp. 291-308, 1984.

28. Ploeg, J. F. and J. H. Duerksen, "Two Successful Steam/Foam Field Tests, Sections 15A and 26C Midway-Sunset Field," *SPE 19609*, Presented at the SPE Calif. Regional Meeting, Bakersfield, March 27-29, 1985.

29. Ruckenstein, E. and R. K. Jain, "Spontaneous Rupture of Thin Liquid Films," *J. Chem. Soc. Faraday Trans. II*, vol. 70, pp. 132-147, 1974.

30. Scheidegger, A. E., *The Physics of Flow Through Porous Media, 3rd ed.*, University of Toronto Press, Toronto, 1974.

31. Taylor, G. I., "Deposition of a Viscous Fluid on the Wall of a Tube," *J. Fluid Mech.*, vol. 10, pp. 161-165, 1961.

32. Teletzke, G. F., "Thin Liquid Films: Molecular Theory and Hydrodynamic Implications," *Ph.D. Thesis*, University of Minnesota, 1983.

33. Williams, M. B. and S. H. Davis, "Nonlinear Theory of Film Rupture," *J. Coll. Int. Sci.*, vol. 90, no. 2, pp. 220-228, 1982.

Appendix A: Conjoining/Disjoining Pressure in Film Deposition

The film-profile equation predicting the deposited film thickness as a bubble displaces a perfectly wetting fluid was first enunciated by Bretherton (1961). Bretherton, and more recently Teletzke (1983), considered role of conjoining/disjoining pressure on the deposited film thickness. The film-profile equation is an approximation valid for $Ca \rightarrow 0$. Park and Homsy (1984) have shown formally, neglecting conjoining/disjoining forces, that Bretherton's solution is the leading order term in an asymptotic expansion in $Ca^{1/3}$. Park and Homsy clarified the characteristic length scales in this problem. To obtain the scaled film-profile equation, we follow Park and Homsy by substituting into Bretherton's profile equation for the dimensional position x^* the scaled length $\tilde{x} = (x^*/R_T^*)/Ca^{1/3}$, and for the dimensional film thickness h^* the scaled thickness $\tilde{h} = (h^*/R_T^*)/Ca^{2/3}$ to yield:

$$\frac{d^3\tilde{h}}{d\tilde{x}^3} - 3\tilde{A}\frac{1}{Ca^2}\frac{1}{\tilde{h}^4}\frac{d\tilde{h}}{d\tilde{x}} = 3\left(\frac{\tilde{h} - \tilde{h}_o}{\tilde{h}^3}\right) \tag{A-1}$$

where $\tilde{h}_o$ is the scaled deposited film thickness. Conjoining/disjoining forces are important when the coefficient multiplying the second term of Equation A-1 is of order one or greater:

$$3|\tilde{A}|\,Ca^{-2} \geq O(1) \quad . \tag{19}$$

This criterion predicts well the onset of conjoining/disjoining forces in Teletzke's (1983) calculation of the deposited film thickness using the conjoining/disjoining pressure functions given by Equation 7.

Table 1

Role of Wettability on Thin-film Breakup

($\tilde{A} = A^*/\sigma R_T^{*2}$)

Partial Nonwetting, $\pi \geq \theta \geq \pi/2$ (Conjoining Pressure $\tilde{A} < 0$)			
Film Deposition (Laydown)	$Ca < \lvert 3\tilde{A} \rvert^{1/2}$ NO	$Ca > \lvert 3\tilde{A} \rvert^{1/2}$ YES	
Snap-off (Evolution)	NO	$Ca < \lvert 3\tilde{A} \rvert^{3/8}$ NO	$Ca > \lvert 3\tilde{A} \rvert^{3/8}$ YES
Perfect Wetting, $\theta = 0$ (Disjoining Pressure $\tilde{A} > 0$)			
Film Deposition (Laydown)	$Ca < (3\tilde{A})^{1/2}$ YES	$Ca > (3\tilde{A})^{1/2}$ YES	
Snap-off (Evolution)	NO	$Ca < (3\tilde{A})^{3/8}$ NO	$Ca > (3\tilde{A})^{3/8}$ YES

Figure Titles

Figure 1. Pore level view of bubble generation by snap-off.

Figure 2. Schematic of a stable collar (a) and a liquid lens (b).

Figure 3. Liquid film wetting the inside wall of a constricted capillary.

Figure 4. Thin-film growth rate for an initial sinusoidal disturbance in a straight cylindrical capillary.

Figure 5. Initial condition of a uniform film thickness.

Figure 6. Profiles for liquid-film evolution in a constricted capillary.

Figure 7. Effect of the initial film thickness and $\tilde{A}$ on the time to break-up; $\tilde{A} > 0$ gives a perfectly wetting liquid, while $\tilde{A} < 0$ indicates a nonwetting liquid. Open circles indicate the onset of dry patch formation.

Figure 8. Profiles for liquid-film evolution with disjoining pressure in a constricted capillary.

Figure 9. Dewetting film due to conjoining pressure.

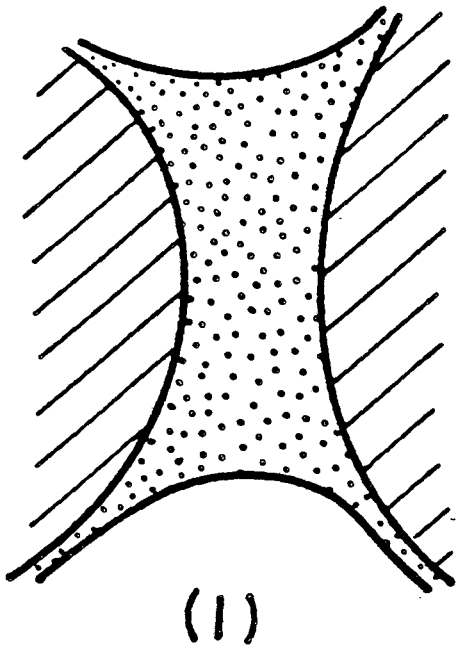

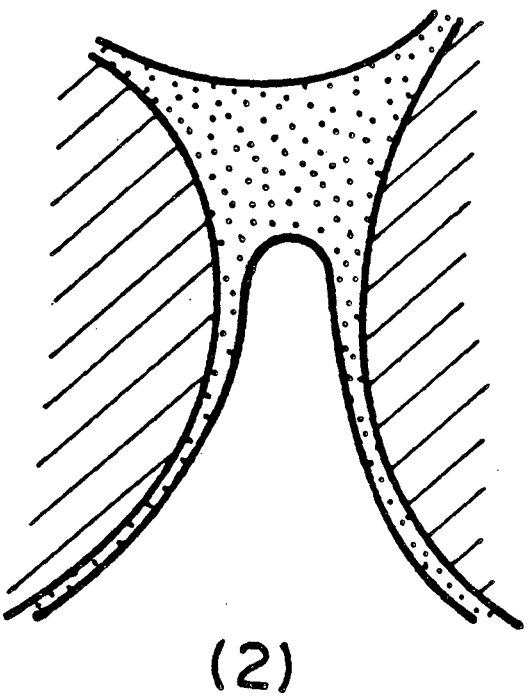

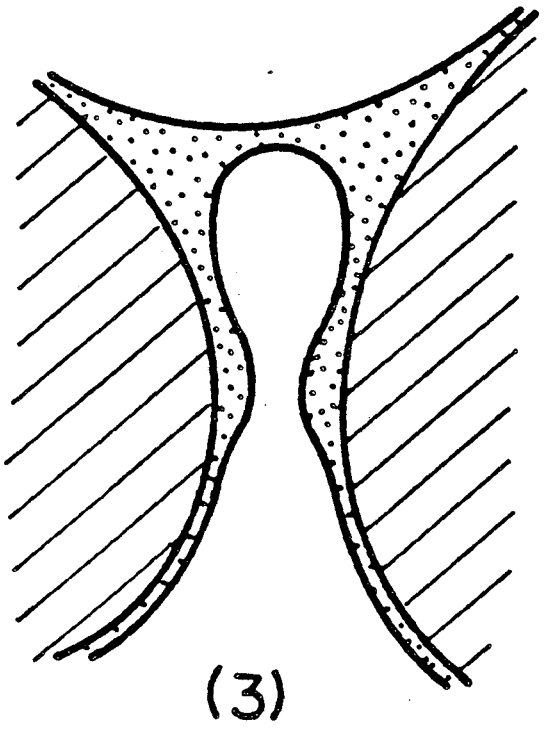

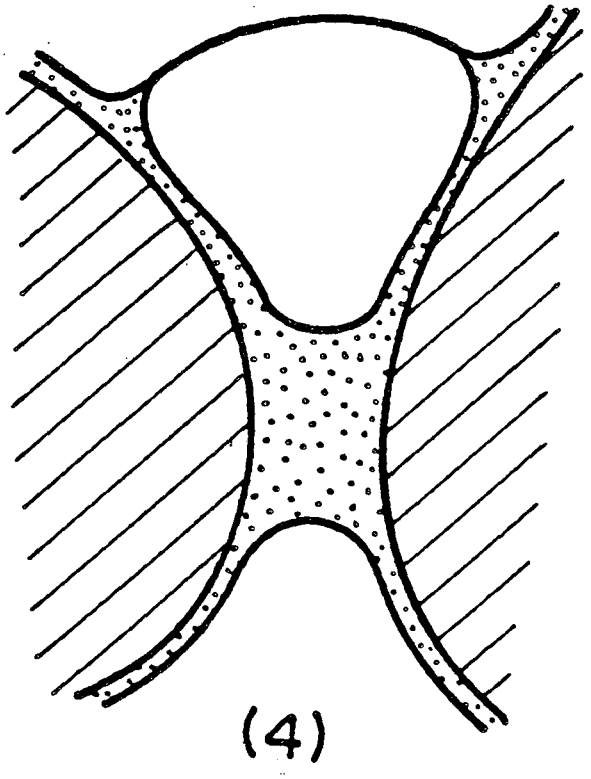

Figure 1

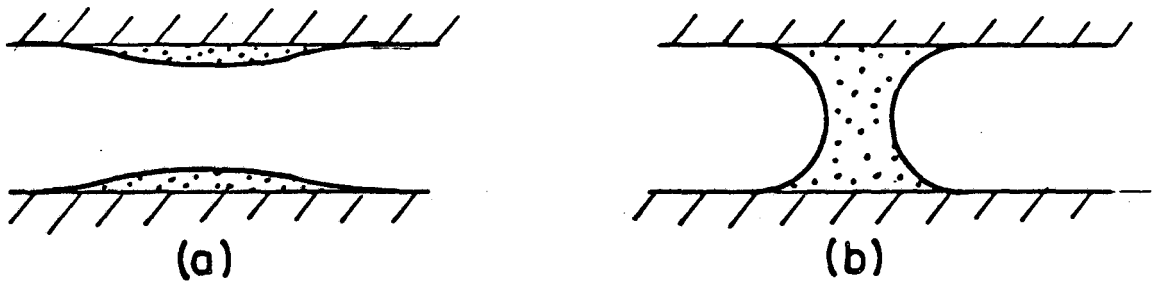

Figure 2

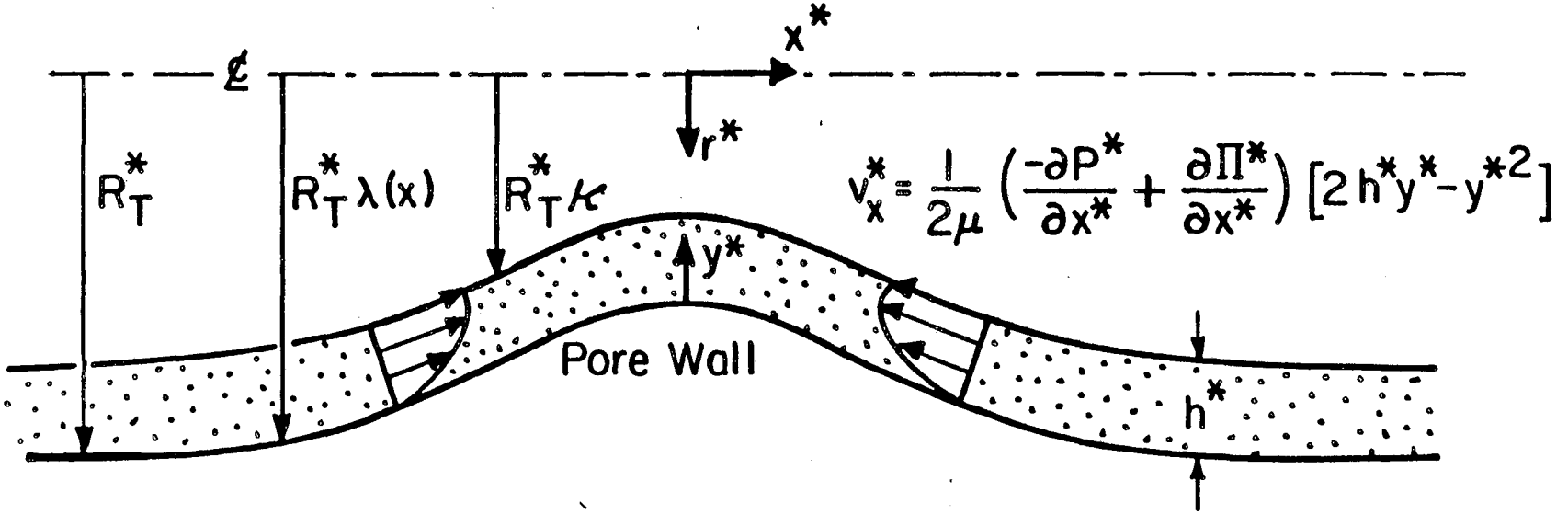
x*
r*
R_T^*
$R_T^*\lambda(x)$
$R_T^*\kappa$
$v_x^* = \frac{1}{2\mu}\left(\frac{-\partial P^*}{\partial x^*} + \frac{\partial \Pi^*}{\partial x^*}\right)[2h^*y^* - y^{*2}]$
y*
Pore Wall
h*

Figure 3

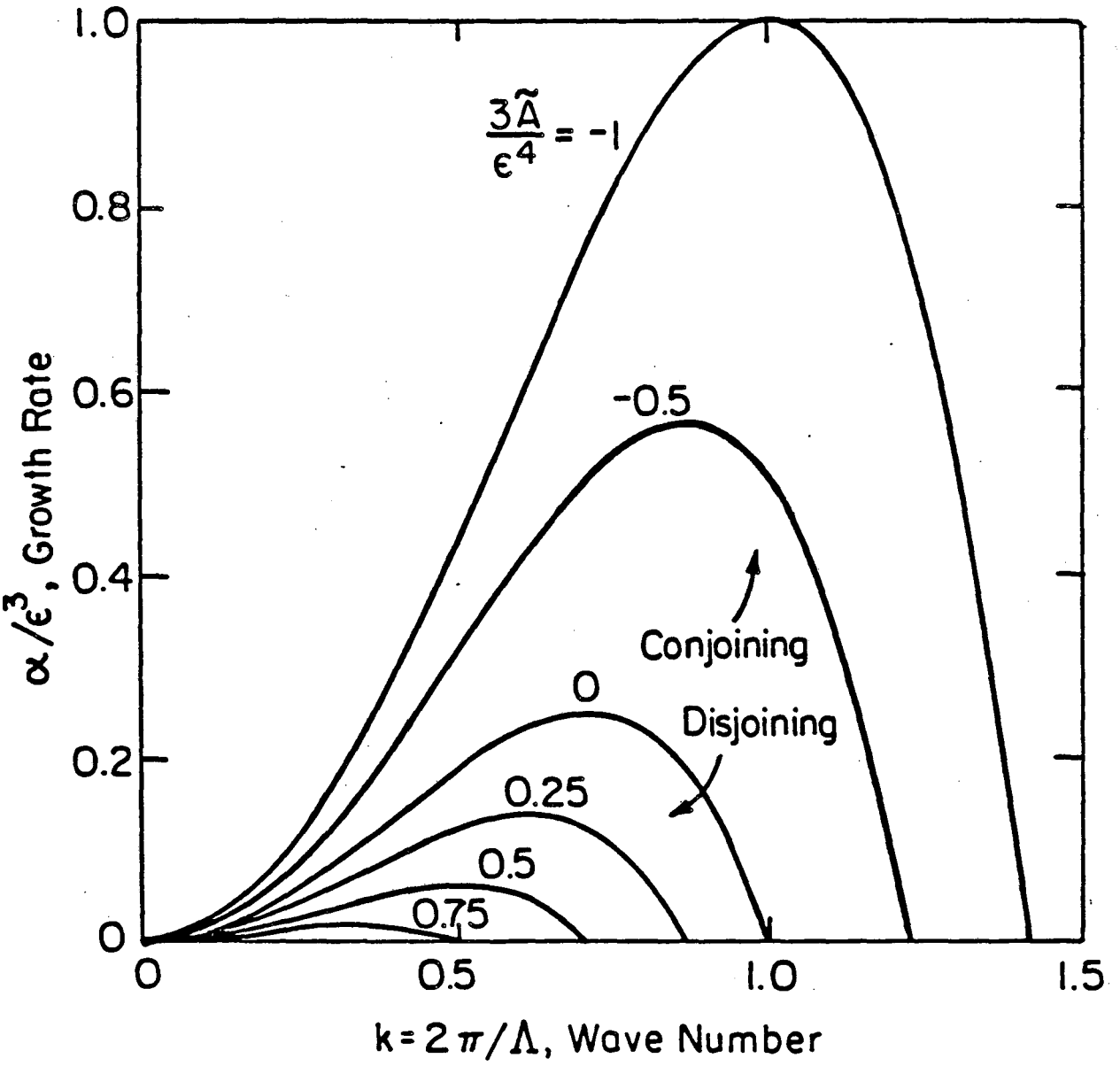
1.0
0.8
0.6
0.4
0.2
0
0
0.5
1.0
1.5
α/ϵ^3, Growth Rate
$k = 2\pi/\Lambda$, Wave Number
$\frac{3\tilde{A}}{\epsilon^4} = -1$
-0.5
0
0.25
0.5
0.75
Conjoining
Disjoining

Figure 4

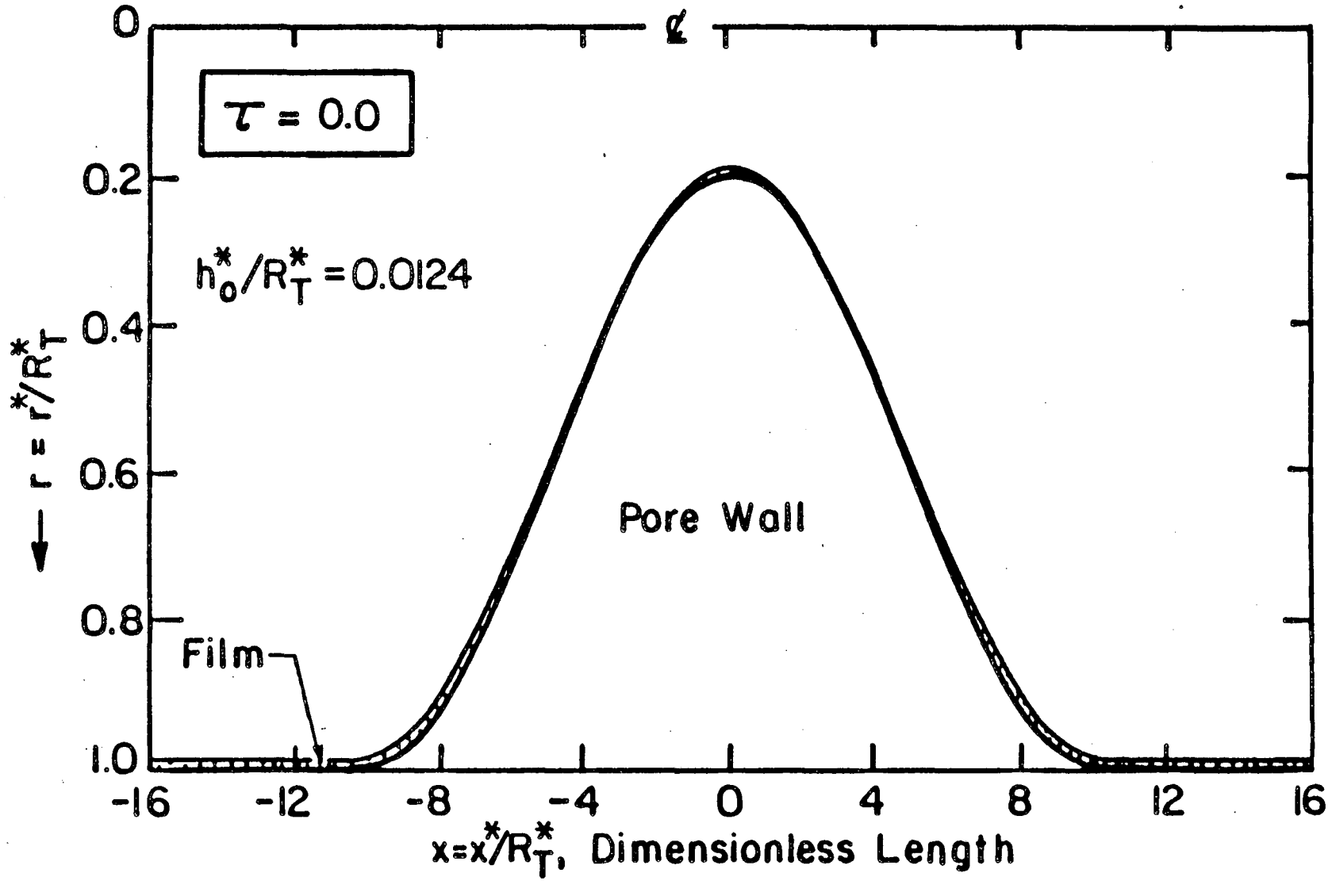
0
ℓ
τ = 0.0
0.2
$h_0^*/R_T^* = 0.0124$
0.4
$r = r^*/R_T^*$
0.6
Pore Wall
0.8
Film
1.0
-16
-12
-8
-4
0
4
8
12
16
$x = x^*/R_T^*$, Dimensionless Length

Figure 5

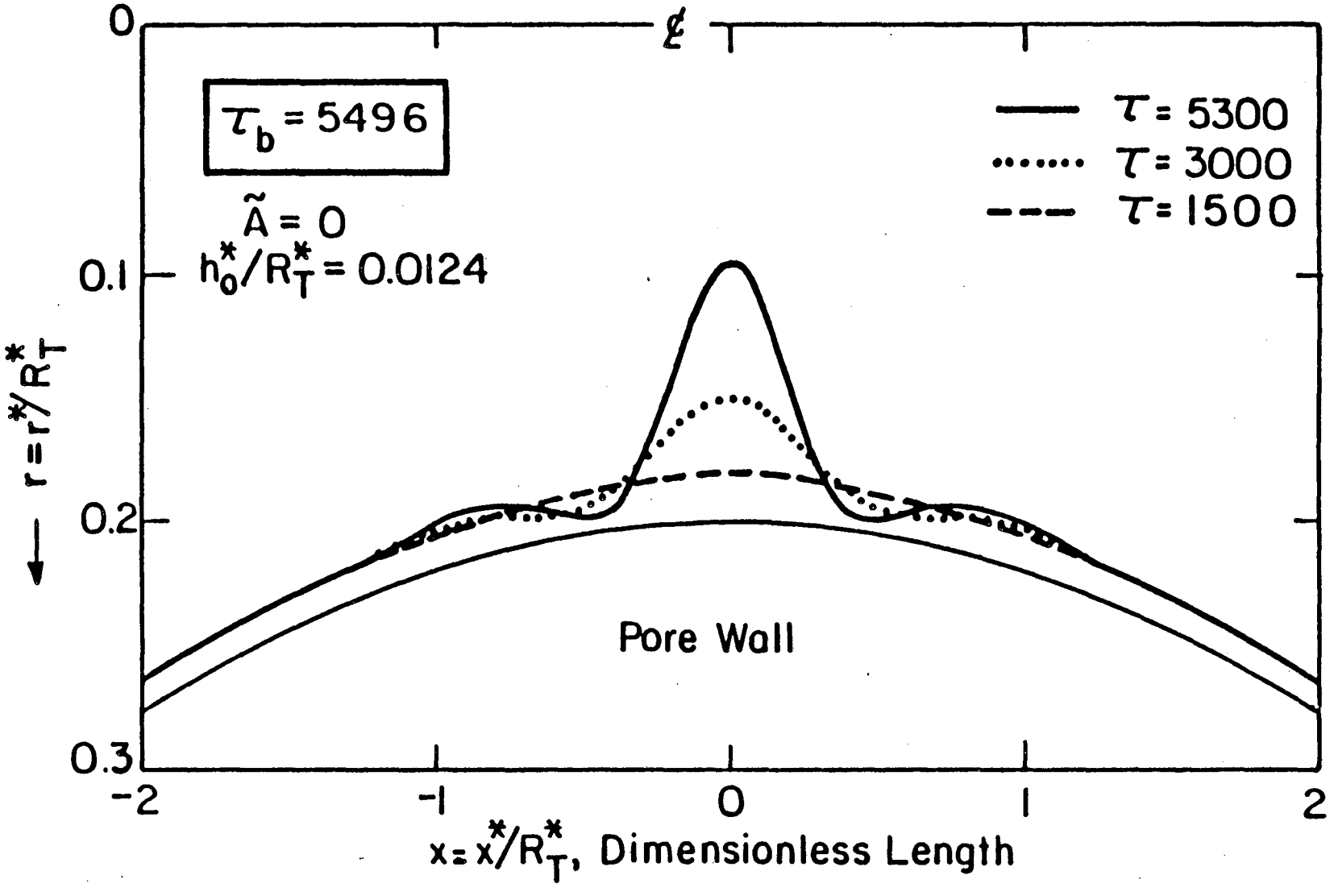
0
ℓ
$\tau_b = 5496$
$\tilde{A} = 0$
$h_0^*/R_T^* = 0.0124$
$\tau = 5300$
$\tau = 3000$
$\tau = 1500$
0.1
0.2
0.3
$r = r^*/R_T^*$
Pore Wall
-2
-1
0
1
2
$x = x^*/R_T^*$, Dimensionless Length

Figure 6

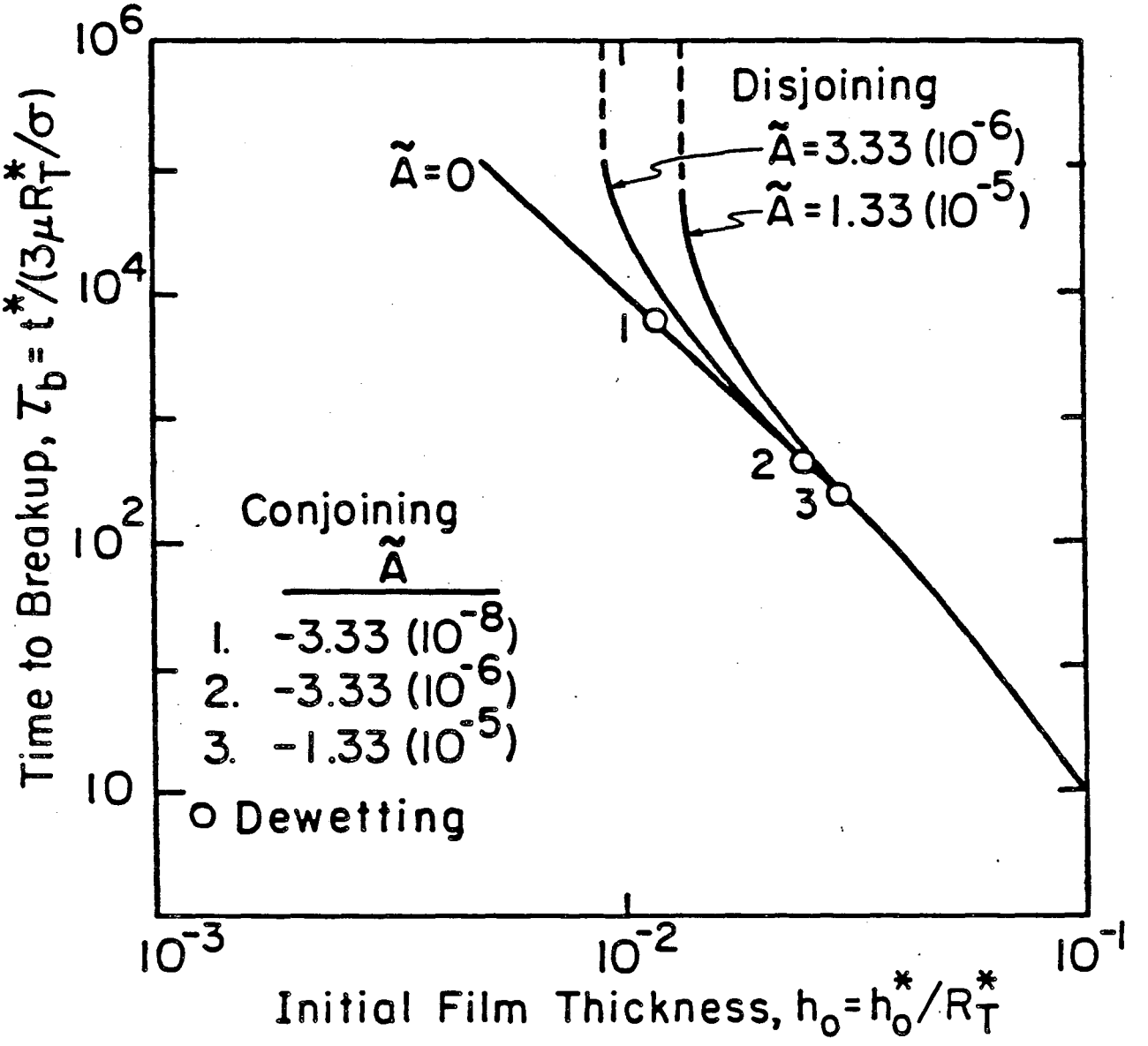
Disjoining
$\tilde{A}=3.33\,(10^{-6})$
$\tilde{A}=1.33\,(10^{-5})$
$\tilde{A}=0$
1
2
3
Conjoining
$\tilde{A}$
1. $-3.33\,(10^{-8})$
2. $-3.33\,(10^{-6})$
3. $-1.33\,(10^{-5})$
o Dewetting
10^{6}
10^{4}
10^{2}
10
10^{-3}
10^{-2}
10^{-1}
Time to Breakup, $T_b = t^*/(3\mu R_T^*/\sigma)$
Initial Film Thickness, $h_o = h_o^*/R_T^*$

Figure 7

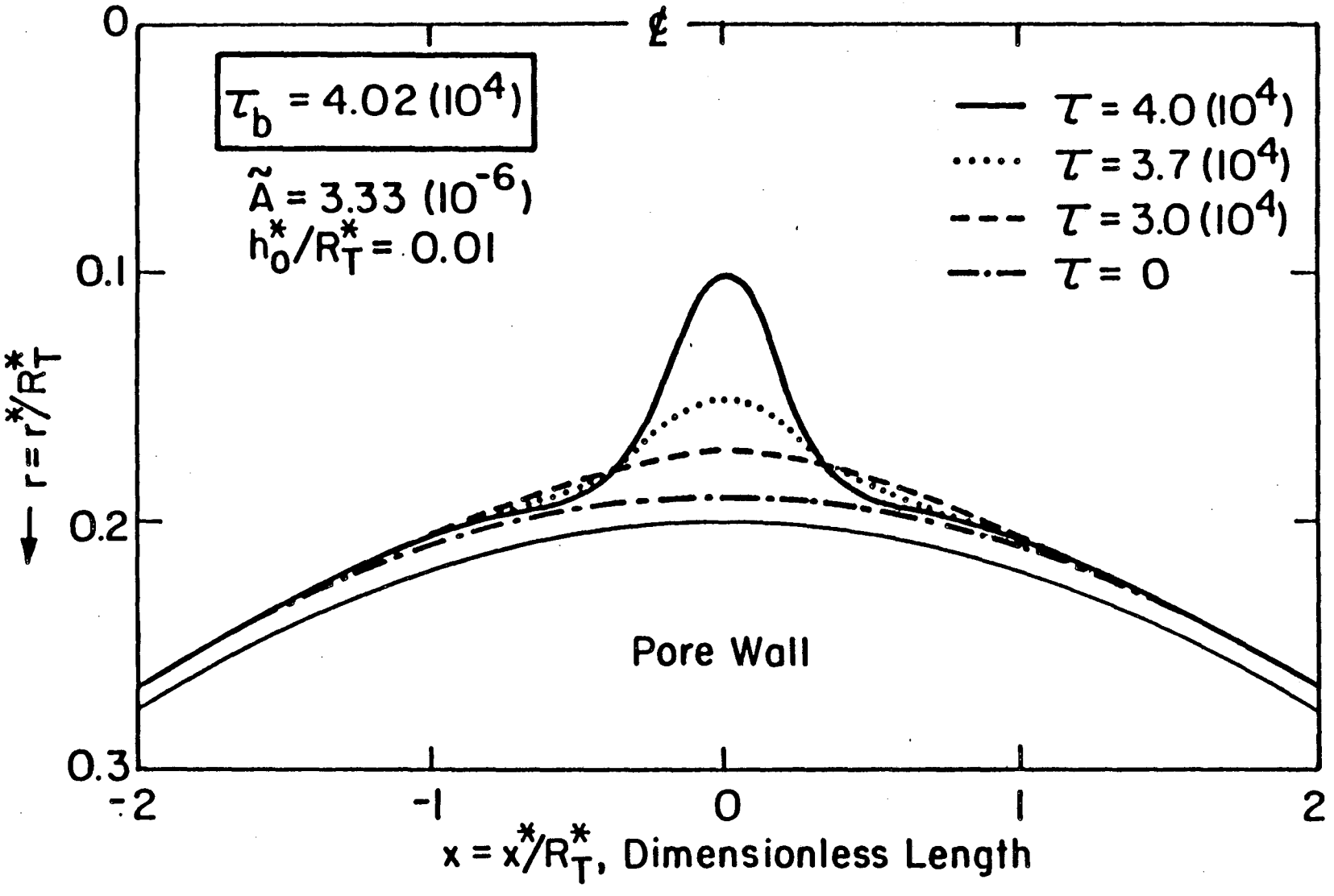
0
℄
$\tau_b = 4.02\,(10^4)$
$\tilde{A} = 3.33\,(10^{-6})$
$h_0^*/R_T^* = 0.01$
$\tau = 4.0\,(10^4)$
$\tau = 3.7\,(10^4)$
$\tau = 3.0\,(10^4)$
$\tau = 0$
0.1
0.2
0.3
$r = r^*/R_T^*$
Pore Wall
-2
-1
0
1
2
$x = x^*/R_T^*$, Dimensionless Length

Figure 8

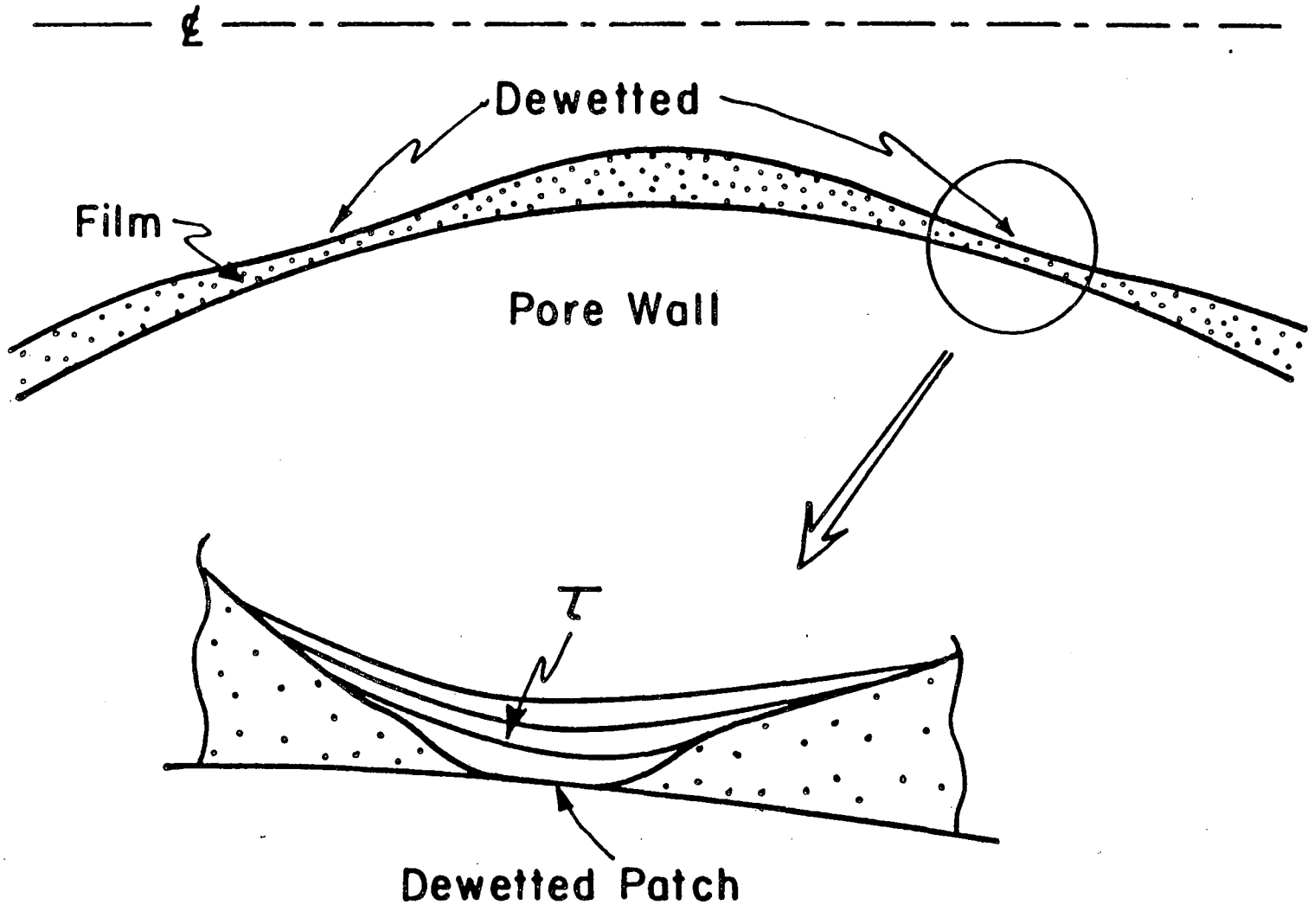

Figure 9

LAWRENCE BERKELEY LABORATORY
TECHNICAL INFORMATION DEPARTMENT
UNIVERSITY OF CALIFORNIA
BERKELEY, CALIFORNIA 94720